ELSEVIER

Biophysical Chemistry 67 (1997) 287–292

Biophysical Chemistry

Dynamic light scattering study of fine semiflexible fibrin networks

Giuseppe Arcovito *, Francesco Andreasi Bassi, Marco De Spirito, Enrico Di Stasio, Michela Sabetta

Instituto di Fisica, Facoltà di Medicina e Chirurgia, Università Catolica S.C., L.go Francesco Vito n. 1, 00168 Roma, Italy

Received 27 January 1997; revised 21 April 1997; accepted 21 April 1997

Abstract

Fine fibrin networks have been investigated using the dynamic light scattering (DLS) technique. At the shortest delay times, t, the dynamic structure factor $s(q,t)$ is found to depend on time according to an exponential function and, at intermediate delay times (up to 1 ms), to a stretched exponential. At longer times ($t > 1$ ms), a progressively increasing deviation from the stretched exponential behaviour has been observed. These results are in agreement with the theoretical predictions of a recently forwarded model for semiflexible polymers in semidilute solutions [K. Kroy and E. Frey, Physical Review E 55 (1996) p. 3092.], despite the fact that fibrin networks are made up of crosslinked branched polymers. The model, moreover, allows the calculation from the initial decay rate $\Gamma_q^{(0)}$ of the average diameter of the fibrin fibres, a. The value of $a = 30 \pm 2$ nm, at fibrinogen concentration $c_f = 1676$ nM and ionic strength 0.5, fits well into the data reported in electron microscopy studies. A concentration dependence of the average diameter of the fibrin fibres has been observed which saturates at the highest concentrations. The diameter of fibrin fibres is an important component in determining the physical properties of the fibrin networks, since the radial growth of fibrin fibres is limited by twisting during protofibrils aggregation. Our results indicate the importance of taking into account intrinsic semiflexibility in studying the physical properties of 'real' polymers and emphasize the high sensitivity of the DLS technique to investigate biological polymers also at the lowest concentrations where the systems are very fragile. © 1997 Elsevier Science B.V.

Keywords: Fibrin; Polymer gel; Dynamic light scattering; Biological network

1. Introduction

The important role played by fibrin clots in a number of pathophysiological processes, such as haemostasis, thrombosis, infection, tumour growth, etc., is well known by now [1]. It has been shown in Refs. [2,3] that a fibrin clot is a gel made up by a network of fibrin fibres grown in a solution of fibrinogen activated by thrombin. Fibrinogen is a rod-shaped protein 340 kD in molecular weight, 45 nm in length and 9 nm in diameter, consisting of three pairs of polypeptide chains $(A\alpha B\beta\gamma)_2$. Upon cleavage of the A and B fibrinopeptides with thrombin, a fibrin monomer is obtained that has two unmasked binding sites in the central domain fitting complementary sites already present in domains at the ends of each molecule. Then, two-stranded protofibrils are formed which aggregate laterally to yield fibrin fibres.

* Corresponding author. Tel. and fax: +39-6- 3013858; e-mail: arcovito@axcasp.caspur.it

PII S0301-4622(97)00056-2

The polymerization mechanism [4–6], as well as the physical properties of this system near the critical sol–gel transition point [7], have been already studied. The gel phase has also been investigated mainly from a macroscopic point of view [8], by measuring viscoelastic gel properties, even when a nonperturbative microscopic probe such as dynamic light scattering (DLS) technique was employed [9]. However, the internal dynamics of fibrin polymers in semidilute solutions is still not well understood. On the other hand, the Gaussian chain model [10–12] used to describe the static and dynamic properties of flexible polymers fails in analysing the light scattering experimental data from fibrin networks because, although fibrin polymers as a whole look rather flexible, they have a local semiflexible structure that cannot be neglected.

Several models have been developed for the elasticity and for the dynamics of semiflexible polymers networks at the intermediate time scales of interest [13,14]. In particular, the model reported in Ref. [14], useful to analyze dynamic light scattering data, has been successfully tested in studying entangled F-actin fibres solutions [15]. The model accounts for the physical properties of specific fibres, such as contour length, persistence length, flexibility, bending and friction coefficient and allows to obtain the average diameter of fibrin fibres from the initial slope of the scattered intensity autocorrelation function.

The present work reports dynamic light scattering measurements on fibrin gels. High NaCl concentrations buffer was used in order to obtain networks of fine fibres with a narrow diameter distribution [8,16]. The results are compared with the theoretical predictions. The average diameter of fibrin fibres has been also determined as a function of fibrinogen concentration.

2. Theoretical background

The dynamic structure factor of polymers in solution is defined in Ref. [17] as:

$$s\left(\underset{\sim}{q},t\right) = \frac{1}{N}\sum_{n,m,\alpha,\beta}\left\langle \exp\left\{ i\,\underset{\sim}{q}\cdot\left[\underset{\sim}{R}_n^{\alpha}(0) - \underset{\sim}{R}_m^{\beta}(t)\right]\right\}\right\rangle \tag{1}$$

where $\underset{\sim}{q}$ is the scattering wave vector. The summation is performed on all pairs n,m of monomers belonging to all polymers α,β at position $\underset{\sim}{R}$ and the brackets denote the ensemble average over all polymer conformations.

In semidilute solutions, the dynamic structure factor of flexible polymers with radii of gyration large compared to length scale, q^{-1}, and with strong hydrodynamic coupling between monomers (Rouse–Zimm chain), has been calculated by Dubois–Violette and de Gennes [10,12] as follows: for $\Gamma_q^{(0)}t \ll 1$

$$s\left(\underset{\sim}{q},t\right) \propto \exp(-\Gamma_q t) \tag{2}$$

and for $\Gamma_q^{(0)}t \ll 1$

$$s\left(\underset{\sim}{q},t\right) = \exp\left\{-1.35\left(\Gamma_q t\right)^{2/3}\right\} \tag{3}$$

where $\Gamma_q^{(0)}$ is the initial slope of the dynamic structure factor and the decay rate Γ_q is given by:

$$\Gamma_q = \frac{k_B T}{6\pi\eta}q^3 \tag{4}$$

As proven in Ref. [18], these theoretical predictions do not fit the experimental data obtained from dilute and semidilute solutions of semiflexible polymers, i.e., from systems fulfilling the conditions:

$$a < q^{-1} < \xi < L_p, L \tag{5}$$

where a is the average diameter of fibrin fibres, ξ the gel mesh size, L_p the persistence length and L the contour length.

For these systems, the model of Ref. [14], assuming that the internal configurational dynamics dominate over the centre of mass and the rotational motions, and in the weakly bending rod limit, calculates the dynamic structure factor, $s(q,t)$, to a good approximation with a stretched exponential:

$$s\left(\underset{\sim}{q},t\right) = \exp\left\{-A\left(\Gamma_q t\right)^{3/4}\right\} \tag{6}$$

where the decay rate

$$\Gamma_q = Bq^z \tag{7}$$

with $z = 8/3$, depends, through the prefactor B, on the persistence length, the stiffness and the friction coefficient of the fibres.

Moreover, the initial decay rate, $\Gamma_q^{(0)}$, is calculated as:

$$\Gamma_q^{(0)} = \frac{k_B T}{6\pi^2 \eta} q^3 \left[\frac{5}{6} - \log qa \right] \quad (8)$$

allowing the determination of the effective average hydrodynamic diameter a of semiflexible polymers forming the network independently of the structural properties of the gel.

3. Materials and methods

3.1. Samples

Lyophilized, plasminogen-free, human fibrinogen (Calbiochem, lot B10707 (341576), USA) was used to prepare samples at different concentrations in freshly prepared buffer (50 mM tris, 500 mM NaCl, 1 mM EDTA, 10 U.I./l kir-aprotinin, pH 7.4), divided into aliquots and stored at −20°C.

Just before using, samples were thawed, purified by gel chromatography in sepharose CL-4B (Pharmacia) in a 1 × 100 cm column at room temperature and filtered through a 0.22 μm low-protein absorption sterile filter (Nucleapore). Fibrinogen concentration was spectrophotometrically checked using an extinction coefficient [19] of $E_{(280)} = 1.506$ ml/mg/cm.

Lyophilized human thrombin (Sigma Aldrich, lot 104H9314, Milan, Italy) was rehydrated and equilibrated in the same buffer used for fibrinogen, divided into aliquots of different volume and concentration, stored at −20°C and thawed just before use. In order to activate fibrinogen, human thrombin was used on a constant ratio of 5 U.I. thrombin to 1 mg fibrinogen.

To check for fibrinogen purity degree and activation by FXIII, after light scattering measurements, all the samples were analyzed using SDS-PAGE electrophoresis carried out on 7.5% polyacrilamide gel in the presence of 0.1% SDS which did not show any trace of γ–γ dimers [20].

3.2. Light scattering measurements

Dynamic light scattering measures the normalized time autocorrelation function $g_2(\boldsymbol{q},t)$ of the scattering intensity $I(\boldsymbol{q})$ defined as [21]:

$$g_2(\boldsymbol{q},t) = \frac{\langle I(\boldsymbol{q},0) I(\boldsymbol{q},t) \rangle}{\langle |I(\boldsymbol{q},0)|^2 \rangle} \quad (9)$$

where $\boldsymbol{q} = \frac{4\pi n}{\lambda} \sin\left(\frac{\vartheta}{2}\right)$ is the scattering wave vector at the wavelength λ, n is the sample refractive index, t the delay time and the brackets indicate ensemble average. $g_2(\boldsymbol{q},t)$ can be simply expressed in terms of the dynamic structure factor $s(\boldsymbol{q},t)$ as [18]:

$$g_2(\boldsymbol{q},t) = 1 + \beta |s(\boldsymbol{q},t)|^2 \quad (10)$$

where $\beta \leq 1$ is the coherence factor depending on the geometry of the optical set-up. In the present set-up a value of $\beta = 0.97 \pm 0.02$ was found, supporting the assumption that the light scattered from fibrin networks exhibits Gaussian statistics [21].

Scattering intensity measurements were performed by using the computer-interfaced scattering system ALV-125 (ALV, Langen, Germany) already described in Ref. [22]. A vertically polarized monochromatic light source of $\lambda = 488$ nm from a 800 mW Ar^+ laser (Coherent Innova 70) was used. The sample was contained in a cylindrical quartz cuvette (1 cm diameter) enclosed in a vat filled with toluene as optical matching fluid.

Experiments were performed at 25°C, 6 h after the adding of thrombin (well above the gelling time $t_g \cong 600$ s). Sample temperature was controlled within ±0.05°C by means of a Julabo HC Thermostat and measured with a Pt100 thermometer.

Moreover, the optical detection set-up included a single mode optical fibre and collimator optics in front of the photomultiplier mounted on the rotating arm of the goniometer. Because the optical fibre truly selects a single mode from the scattering field, one obtains the ideal mixing efficiency without having to sacrifice the signal strength [23]. This feature allows the analysis of photons scattered from large scattering volumes ($\cong 1$ mm^3), thus overcoming problems due to the intrinsic nonergodicity of fibre networks. The photopulses were sent to a 256-channel digital autocorrelator (ALV-5000) that performed a hardware autocorrelation function of the pho-

topulses with a logarithmic spacing of delay times starting from 0.2 μs.

Data were collected from several scattering angles (usually eight) ranging from 30° to 135°, corresponding to wave vectors 0.88×10^5 cm$^{-1} \leq q \leq 3.2 \times 10^5$ cm^{-1}.

4. Results

The dynamic structure factors $s(q,t)$ of fibrin networks have been obtained by Eq. (10) from normalized intensity autocorrelation function measurements carried out on samples at different fibrinogen concentration ($c_f = 225$ nM, 872 nM, 1676 nM and 3202 nM).

In order to analyse the asymptotic behaviour of the $s(q,t)$ curves, at the shortest ($\Gamma_q^{(0)} t \ll 1$) and the longest ($\Gamma_q^{(0)} t > 1$) delay times, Fig. 1 reports the log–log plot of the log $[1/s(q,t)]$ versus the delay time t for the sample at $c_f = 3202$ nM. As can be seen, at the shortest time $s(q,t)$ is an exponential function of time: $s(q,t) \propto \exp(-\Gamma t)$, while, at intermediate delay times, $s(q,t)$ is a stretched exponential function, i.e., $s(q,t) \propto \exp[-(\Gamma t)^{\beta}]$ with $\beta = 3/4$ according to Eq. (3). At longer times, an increasingly greater deviation from the predictions of Eq. (3) can be observed. The same results have been

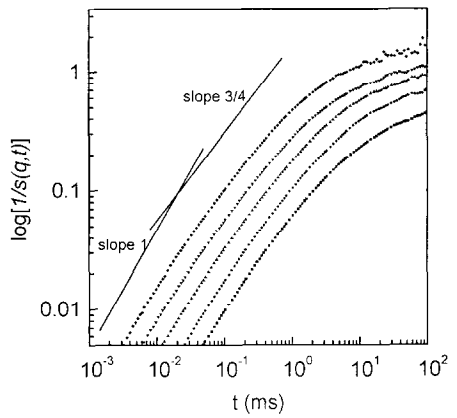

Fig. 1. Log–log plot of log $[1/s(q,t)]$ of a fibrin network at fibrinogen concentration $c_f = 3202$ nM, as a function of the delay time t. The scattering wave vectors were, from left to right, $q = 1.00\ 10^{-5}$ nm^{-1}, $1.14\ 10^{-5}$ nm^{-1}, $1.69\ 10^{-5}$ nm^{-1}, $2.40\ 10^{-5}$ nm^{-1} and $2.89\ 10^{-5}$ nm^{-1}. The drawn lines have slope of 1 and of 3/4.

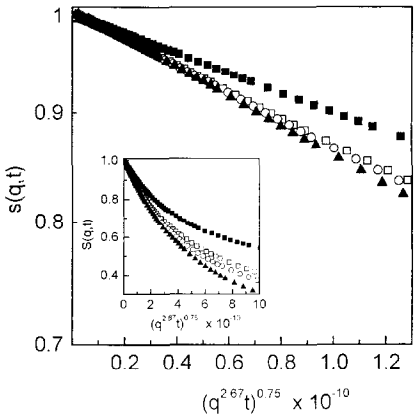

Fig. 2. Plot of the dynamic structure factor $s(q,t)$ of two fibrin networks at concentration 3202 nM (□, ■) and 872 nM (○, ▲), for two scattering wave vectors ($q = 1.2\ 10^{-5}$ nm^{-1} (○, ■) and $q = 1.8\ 10^{-5}$ nm^{-1} (□, ▲)), against the adimensional parameter $(q^{8/3}t)^{3/4}$, up to $t \cong 1$ ms. A superposition of the data is shown, except for the data at 3202 nM and at the scattering angle $\theta = 39°$ ($q = 1.14\ 10^{-5}$ cm^{-1}). In the inset the same data are reported up to delay times $t \cong 10$ ms. For $t > 1$ ms, a marked deviation of all curves from the previous common behaviour clearly appears.

obtained from all the examined samples. Indeed, as shown in Fig. 2, where $s(q,t)$ values for two samples at different concentrations c_f are plotted versus the dimensional parameters $(q^{8/3}t)^{3/4}$, data measured at scattering angle $\theta > 39°$ ($q = 1.14\ 10^{-5}$ cm^{-1}) coincide. At $\theta < 39°$ there is a marked discrepancy from the theoretical predictions of Eq. (3)

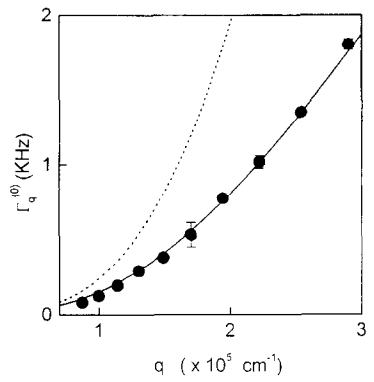

Fig. 3. The initial decay rate $\Gamma_q^{(0)}$ of the dynamic structure factor of a sample at $c_f = 3202$ nM is plotted against the wave vector q. From the fit of Eq. (10) to the experimental data (full line) a value of the average diameter of the fibres $a = 30 \pm 2$ nm has been found. The theoretical prediction for a Gaussian chain (dashed line) is also reported for comparison.

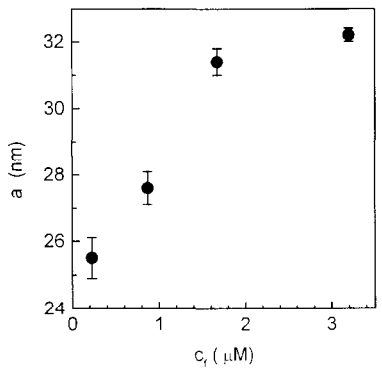

Fig. 4. Plot of a, the average diameter of the fibrin fibres, versus the solution concentration c_f. A saturation behaviour, new to our knowledge, is observed at the highest concentrations.

also on the $\tilde{q}$ dependence for all the examined concentrations. Moreover, as emphasized in the inset of Fig. 2., the long time tails ($t \gg 1$ ms) of all the curves also depart markedly from the theory.

The initial slope of $s(\tilde{q},t)$ has been analyzed by applying the cumulant method [21] to obtain $\Gamma_q^{(0)}$ values as a function of $\tilde{q}$. The results for the sample at $c_f = 3202$ nM are reported in Fig. 3, where it is also shown that Eq. (10) fits well to the experimental data giving a value $a = 32 \pm 5$ nm for the average diameter of the fibrin fibres. In the same Fig. 3, the clear deviation of the experimental data from the behaviour predicted for Gaussian chains is also shown.

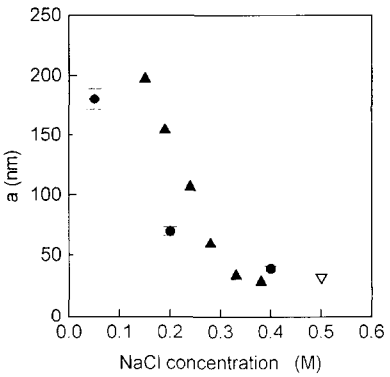

Fig. 5. The average diameter of the fibrin fibre a at $c_f = 1676$ nM and ionic strength 0.5 (▽) is compared with those reported (▲ in Ref. [8] and ● in Ref. [22]) obtained at lower ionic strengths. Our data confirm and extend the range of the saturation regime with ionic strength.

Similar results have been obtained for the other samples at different fibrinogen concentrations. In Fig. 4 the average diameter of fibrin fibres, a, is plotted versus the concentration showing a saturation behaviour at the highest c_f, which emphasizes once more the sensitivity and the accuracy of the DLS technique.

In Fig. 5, the average diameter of the fibrin fibres a of the sample at $c_f = 1676$ nm and at high ionic strength (0.5 M NaCl) is compared with the values measured by other authors [8,16] at the same concentration and at different ionic strengths (up to 0.4 M NaCl). As can be seen, our data fit into and extend the range of the known saturation regime at the highest ionic strength, where the fibre diameters do not change any more.

5. Discussions

In agreement with the results obtained by different experimental techniques [8,18,24,25], it can be assumed that a fibrin polymer is intrinsically semiflexible, i.e., Eq. (5) is fulfilled.

Measurements reported in Figs. 1 and 2 seem to confirm this hypothesis, showing a good agreement of the experimental data with the theoretical predictions, for delay time up to 1 ms. For $t \gg 1$ ms and at $\theta < 39°$, a marked deviation of the $s(\tilde{q},t)$ data from the predicted behaviour is reported.

Similar behaviour observed when analysing the data from semidilute solutions of semiflexible F-actin filaments [13,15,18], was attributed to the coupling of the long wavelength modes of single-chain dynamics to the cooperative motion of the polymers ensemble. Moreover, since fibrin networks are formed by branched crosslinked polymers, they constitute systems more rigid than semidilute solutions of F-actin, and it can therefore be expected that cooperative chain motions will influence the $s(\tilde{q},t)$ behaviour starting from relatively shorter delay times ($\cong 1$ ms).

It is noteworthy to emphasize that a fibrin network is a crosslinked branched polymers system with a relaxation dynamics more complex than that of an entangled semidilute solution of fine filaments of F-actin. In spite of this, the theoretical model still describes correctly the polymers dynamics until the

influence of the motions of the entire network can not be neglected any more.

The determination of the average diameter of the fibrin fibres linked in a network is also an interesting result of our measurements. Indeed, it was demonstrated in Refs. [15,24,25], mainly by electron microscopy, that fibrin fibres are twisted and this twisting has been suggested as an aggregation mechanism which limits the lateral growth of fibres, that is of the fibres diameter. The twisting capability of protofibrils has been related to the flexibility of the fibrin molecules. Increased twist or decreased flexibility will limit the growth of the fibres to a smaller diameter, whereas decreased twist or increased flexibility will allow for thicker fibres. Moreover, it was proved [16] that by increasing the NaCl concentration of the solution, the fibre diameter decreases. At the same time, the probability of branching increases and the fibrin networks, made by straight fibres, are more rigid. In addition, the diameters distribution narrows as the NaCl concentration increases.

The value of the average diameter of fibrin fibres obtained in this work, when compared with those reported as a function of NaCl concentration (up to 0.4 M NaCl), confirms the above model for the gel structure and extends the range of the known saturation regime up to 0.5 M NaCl.

Finally, a decrease of the average diameter of fibrin fibres at the lowest concentration (see Fig. 4) could be interpreted as due to the shift of the reaction equilibrium toward the formation of thinner polymers. Further measurements are in progress to investigate both this hypothesis and the specific influence of Cl^- ions on the fibre sizes, as recently reported in Ref. [26].

Regardless of the physical meaning, this result clearly emphasizes the high sensitivity of the DLS technique to investigate the dynamical properties of soft systems, such as biological gels at low concentrations, where these systems are very fragile.

Acknowledgements

This work was supported by grants from Ministero dell'Università e della Ricerca Scientifica (M.U.R.S.T.), Consiglio Nazionale delle Ricerche (C.N.R.) and Instituto Nazionale per la Fisica della Materia (I.N.F.M.)

References

[1] M.W. Mosesson, R.F. Doolittle (Eds.), Molecular Biology of Fibrinogen and Fibrin, Conference of the Ann. NY Acad. Sci. held on June 2–4, 1982, NY, 1983, pp. 1–602.
[2] R.F. Doolittle, Ann. Rev. Biochem. 53 (1984) 195.
[3] R.R. Hantgan, J. Hermans, J. Biol. Chem. 254 (1979) 11272.
[4] P. Wiltzius, G. Dietler, W. Kanzig, A. Haberli, P.W. Straub, Biopolymers 21 (1982) 2205.
[5] G. Dietler, W. Kanzig, A. Haberli, P.W. Straub, Biopolymers 25 (1986) 905.
[6] W.J. Weisel, Biophys. J. 50 (1986) 1079.
[7] P. Wiltzius, G. Dietler, W. Kanzig, V. Hofman, A. Haberli, P.W. Straub, Biophys. J. 38 (1982) 123.
[8] B. Blomback, K. Carlsson, B. Hessel, A. Liljeborg, R. Procyk, N. Aslund, Biochim. Biophys. Acta 997 (1989) 96.
[9] R.A. Gelman, J.A. Gladner, R. Nossal, Biopolymers 19 (1980) 1259.
[10] E. Duboise-Violette, P.G. de Gennes, Physics 3 (1967) 181.
[11] P.G. de Gennes, Scaling Concept in Polymer Physics, Cornel Univ., Ithaca, NY, 1979.
[12] M. Doi, S.F. Edwards, The Theory of Polymer Dynamics, Oxford Univ. Press, Oxford, 1986, p. 135.
[13] F.C. MacKintosh, J. Käs, P.A. Janmey, Phys. Rev. Lett. 75 (1995) 4425.
[14] K. Kroy, E. Frey, Phys. Rev. E 55 (1996) 3092.
[15] R. Gotter, K. Kroy, E. Frey, M. Barmann, E. Sackmann, Macromolecules 29 (1996) 30.
[16] T.C. Baradet, J.C. Haselgrove, W. Weisel, Biophys. J. 68 (1995) 1551.
[17] M. Adam, M. Delsanti, Contempor. Phys. 30 (1989) 203.
[18] C. Schmidt, M. Barmann, G. Isenberg, E. Sackmann, Macromolecules 22 (1989) 3638.
[19] E. Mihaly, Biochemistry 7 (1968) 208.
[20] S.V. Pizzo, L.M. Taylor Jr., M.L. Schawrtz, R.L. Mill, P.A. McKee, J. Biol. Chem. 248 (1973) 4584.
[21] B. Berne, R. Pecora, Dynamic Light Scattering, Wiley, New York, 1976.
[22] F. Andreasi Bassi, G. Arcovito, M. De Spirito, A. Mordente, G.E. Martorana, Biophys. J. 69 (1995) 2720.
[23] J. Rickä, J. Appl. Opt. 32 (1994) 2860.
[24] J.W. Weisel, C. Nagaswami, L. Makowski, Biophysics 84 (1987) 8991.
[25] J.W. Weisel, C. Nagaswami, Biophys. J. 63 (1992) 111.
[26] A. Vindigni, E. Di Cera, Biochemistry. 35 (1996) 4417.